Characteristic patterns of an inhomogeneous imaging system with an application to vision

L. Sirovich and B. W. Knight

The Laboratory of Biophysics, Rockefeller University, New York, New York 10021

Received August 1, 1983; accepted September 25, 1985

We examine consequences of image-forming inhomogeneity in the form of a point-spread function that changes with position on the image plane. The familiar self-replicating sinusoids, which a homogeneous system simply multiplies by its spatial modulation-transfer function, generalize to eigenfunctions, which the system multiplies by eigenvalues. We give a way to calculate the eigenfunctions and eigenvalues from the variable point-spread function. We illustrate this with data from the visual system and show that these lead to a discrete set of most-sensitive eigenfunctions, which we construct.

1. INTRODUCTION

Analyses of vision must include some consideration of the consequences of retinal inhomogeneity. The intercone spacing, the interganglion cell distances, and therefore the natural space scale of the retina are smallest in the fovea and increase by large factors in the periphery and far periphery of the retina. Such inhomogeneity has yet to be taken into account in theories of spatial vision. This paper presents a theory of linear, spatially inhomogeneous transformations, motivated by the problem of analyzing the effects of retinal inhomogeneity.

In general we show new features that emerge in the performance of any imaging system that is inhomogeneous in the sense that its point-spread function changes in shape at different places on the image plane. In a system for which this inhomogeneity is important it is no longer possible to characterize imaging performance in terms of the usual spatial modulation-transfer function, which simply attenuates sine waves according to their spatial frequency.[1-3] However, we will show how one still may find *characteristic object patterns* that reappear as image patterns unaltered except in contrast, and we will show how that contrast change may be calculated. Unlike the case of a homogeneous imaging system, we will see that such characteristic patterns may form a discrete set. The application to the human visual system is presented in Sections 4 and 5.

The sort of transformation explored here is given by

$$r(\mathbf{x}) = \int \mathrm{d}\mathbf{y} K\{\mathbf{x}, \mathbf{y}\} e(\mathbf{y}) \tag{1}$$

between the object's distribution of brightness $e(\mathbf{y})$ at points $\mathbf{y}$ (in two dimensions for simplicity) and an image whose intensity is $r(\mathbf{x})$ at corresponding points $\mathbf{x}$. The transformation kernel (or point-spread function) $K\{\mathbf{x}, \mathbf{y}\}$ specifies how the intensity at each point of the input is weighted at each point of the output. A transformation of the type of Eq. (1) is *linear* in the sense that it respects superposition: Weighted and summed inputs yield corresponding weighted and summed outputs: for constants a and b,

$$e_1(\mathbf{y}) \to r_1(\mathbf{x}),$$

$$e_2(\mathbf{y}) \to r_2(\mathbf{x}) : ae_1(\mathbf{y}) + be_2(\mathbf{y}) \to \mathrm{a}r_1(\mathbf{x}) + br_2(\mathbf{x}). \tag{2}$$

Under mild and reasonable conditions on K, transformations of the type of Eq. (1) generically possess characteristic functions, each of which replicates itself under transformation with a characteristic size change λ:

$$\int \mathrm{d}\mathbf{y} \mathrm{K}\{\mathbf{x}, \mathbf{y}\}\psi(\mathbf{y}) = \lambda\psi(\mathbf{x}), \tag{3}$$

and generically such eigenfunctions compose a set complete enough so that any reasonable object function $e(\mathbf{y})$ may be expressed as a linear superposition of them. In the special case of a *spatially homogeneous* transformation $\mathrm{K}\{\mathbf{x}, \mathbf{y}\} = K\{\mathbf{x}-\mathbf{y}\}$, the eigenfunctions are (for arbitrary real vector $\mathbf{p}$ and constant A)

$$\psi(\mathbf{y}) = A \exp(i\mathbf{p} \cdot \mathbf{y}), \tag{4}$$

whose corresponding eigenvalues are

$$\lambda = \int \mathrm{d}\mathbf{u} K(\mathbf{u}) \exp(-i\mathbf{p} \cdot \mathbf{u}), \tag{5}$$

as substitution of Eq. (4) into Eq. (3) shows. Equations (4) and (5) summarize the familiar spatial-modulation transfer-function approach to characterizing an imaging system in terms of response to spatial sine waves[4] and assume that the point-spread function $K\{\mathbf{x}, \mathbf{y}\}$ is the same function of only two-point separation throughout the image plane. Below we present the appropriate generalization of Eqs. (4) and (5) to the much more broadly applicable situation in which the point-spread function changes only slightly *within its own spread* but may undergo major changes across the whole image plane.

As an illustrative example we will present an application to the human visual nervous system. Over the visual field, which extends across about 180 deg, its psychophysical point-spread function undergoes orders-of-magnitude changes, and although a proper experiment shows inhomogeneity already at about 1/2 deg from the center of best

0740-3224/86/030358-07$02.00

resolution, the limit of resolution there indicates a point-spread function an order of magnitude narrower. The requirements of our procedure are fulfilled.

The application of linear Eq. (1) to the human visual response deserves comment beyond the observation that the spatial transfer function method, which assumes this relation, has had a long history of success in numerous visual applications. Quite generally, any rule that gives smooth change in output for smooth change in input and null output for null input may be shown[5] to satisfy an expression of the form

$$r(\mathbf{x}) = \int d\mathbf{y} K_1\{\mathbf{x}, \mathbf{y}\} e(\mathbf{y}) + \iint d\mathbf{y}_1 d\mathbf{y}_2 K_2\{\mathbf{x}, \mathbf{y}_1, \mathbf{y}_2\} e(y_1) e(\mathbf{y}_2) + \iiint d\mathbf{y}_1 d\mathbf{y}_2 d\mathbf{y}_3 \ldots, \tag{6}$$

for which Eq. (1) is a first approximation that retains the leading term. More forcefully, if in addition the quantitative rule under examination transforms spatially uniform input to uniform output, and if we let $e(\mathbf{y})$, $r(\mathbf{x})$ be the *departures* from those uniform conditions, then Eq. (6) *still* holds with K_1, K_2, etc. now dependent on that uniform input from which $e(\mathbf{y})$ departs. Again Eq. (1) is a leading-term approximation with $K\{\mathbf{x}, \mathbf{y}\}$ now dependent on the average intensity of the object. Such an approximation has in fact led to extremely accurate detailed predictions of the measured neutral response in an invertebrate visual system.[6–12]

Equation (1) is fully compatible with the numerous studies on subjective scaling of contrast[13–17] in which subjects choose a wide variety of nonlinear (including linear) subjective scales for contrast, depending on experimental conditions. In these experiments the subject is faced with an additional judgment of how to apply the scale, which choice (in the absence of highly influential advice, like "scale these contrasts logarithmically") is made in a manner highly dependent on what is shown.

The general linear relation (1) may be tried (and has been) under a wide variety of circumstances encompassing many different ways in which the observer quantifies what he sees. For illustrative purposes, we apply it below to two separate somewhat speculative channel mechanisms isolated by fairly involved experimental paradigm[18,19] in which inhomogeneity appears (see also Refs. 20–23). We do this in the spirit that a lucid procedure for treating measurements, even when applied in conjuction with a still maturing theory such as the channel model, can nonetheless further our ultimate undertaking by arranging the experimental facts with a different perspective.

2. FORMULATION

In keeping with experiment we consider a one-dimensional caricature of Eq. (1):

$$r(x) = \int K\{x, y\} e(y) dy. \tag{7}$$

In writing Eq. (7) or Eq. (1) we suppress a time variable since dynamics will not be considered in this paper. We make the further approximation, in part borne out by experience, of the reciprocity of cause and effect, namely, that a unit stimulus at y elicits at x the same response that a unit stimulus at x produces at y. As a result, K is symmetric:

$$K\{x, y\} = K\{y, x\}, \tag{8}$$

and without loss of generality we may write

$$K\{x, y\} = K(x-y, (x+y)/2), \tag{9}$$

which from Eq. (8) is symmetric in the first argument.

As mentioned in the introduction, homogeneity is an approximation; the more accurate picture is one that includes the slow departure from homogeneity. Formally, such a two-scale situation is represented by a kernel having the form

$$K\{x,y\} = K(x-y, \epsilon(x+y)/2), \tag{10}$$

where ϵ is a small parameter. The channel models of Wilson and Bergen[19] can be put in the framework of Eq. (10). A typical kernel of theirs is represented as a difference of Gaussians,

$$K = \frac{A_0}{1+a|\bar{x}|}\left\{\exp\left[-\frac{(\bar{x}-\bar{y})^2}{\sigma^2(1+k|\bar{x}|)^2}\right] - B\exp\left[-\frac{(\bar{x}-\bar{y})^2}{b^2\sigma^2(1+k|\bar{x}|)^2}\right]\right\}. \tag{11}$$

Spatial variables $\bar{x}$ and $\bar{y}$ carry an overbar in anticipation of the renormalization that is given below. The space constants, which measure the resolution of the system, are seen to vary linearly. In general, inhibition occurs over a broader scale so $b > 1$. The relative balance of excitation and inhibition is measured by the constant B. Finally, we note that the amplitude (or sensitivity) of the mechanism decreases inversely with distance.

It proves useful to normalize with respect to a natural scale of the network; in this case the space constant σ is appropriate. Thus we write

$$x = \bar{x}/\sigma, \qquad y = \bar{y}/\sigma \tag{12}$$

and also set

$$\epsilon = k\sigma, \qquad \kappa = k/a. \tag{13}$$

From the values reported in Ref. 19, ϵ is typically $0(10^{-2})$. (See Table 1.)

We see that Eq. (11) is not in symmetric form. To repair this, observe first that both terms of Eq. (11) are peaking functions in $x-y$ and hence fall off rapidly when the magnitude of this difference increases. Secondly, we observe

$$\epsilon|x| = \epsilon\left|\frac{x+y}{2}\right| + 0[\epsilon(x-y)].$$

It therefore follows that $\epsilon|x|$ can be replaced by $\epsilon|x+y|/2$ in Eq. (11). The result is

Table 1. Parameter Values

	κ	ϵ	A_0	σ	k
N mechanism	0.543	0.0035	865	0.028 deg	0.125
S mechanism	0.321	0.0068	1275	0.055 deg	0.125

$$K = \frac{A_0}{1+\epsilon|x+y|/(2\kappa)}\left\{\exp\left[-\frac{(x-y)^2}{(1+\epsilon|x+y|/2)^2}\right] - \frac{1}{\sqrt{3}}\exp\left[-\frac{(x-y)^2}{3(1+\epsilon|x+y|/2)^2}\right]\right\}. \quad (14)$$

For convenience we have taken $B = \sqrt{3}$ and $b^2 = 3$, which in fact lie quite close to the measured values for the so-called S and N mechanisms of Ref. 19.

3. EIGENFUNCTION THEORY

The eigenfunction analysis for kernels of the type of Eqs. (10) and in particular (14) does not generally yield exact results. Nevertheless a highly accurate approximate analysis, based on the WKB method,[24,25] can be performed, the details of which can be found elsewhere.[26–28]

The eigenfunctions and corresponding eigenvalues of Eq. (10) are defined by

$$\int K\left[x-y, \frac{\epsilon}{2}(x+y)\right]\psi(y)dy = \lambda\psi(x). \quad (15)$$

An approximate representation of ψ can be obtained in the form

$$\psi \sim \mathcal{A}(q)\exp\left[\frac{i}{\epsilon}\int^q p(s)ds\right]; \qquad q = \epsilon x. \quad (16)$$

After expression (16) is introduced into Eq. (15), an asymptotic analysis shows that $p(q)$ is defined implicitly by

$$\lambda = \tilde{K}(p,q) = \int K(u,q)\exp[-ipu]du, \quad (17)$$

in which $K(u, q)$ is the kernel that appears in Eq. (15). The eigenvalue λ is defined by the condition that the area included inside a contour in the (p, q) plane defined by Eq. (17) and denoted by $A(\lambda)$ is such that

$$A(\lambda) = (2n+1)\pi\epsilon, \quad (18)$$

where n is a nonnegative integer. The amplitude coefficient of expression (16) is then given by

$$\mathcal{A}(q) = |\tilde{K}_p[p(q), q]|^{-1/2}. \quad (19)$$

Thus the entire structure of the eigenfunction (16), including the value of the eigenvalue λ, follows from examining $\tilde{K}(p, q)$. $\tilde{K}$ is defined by Eq. (17) and is termed the Wigner transform of K. It is important to note that in view of symmetry (8), $\tilde{K}$ is a real function, and the construction is well defined.

Before turning to an explicit calculation we remark on two aspects of our deliberations that bear on (1) how measurements are made and (2) the phenomenon of cortical magnification.

In view of the assumed smallness of ϵ it might be supposed that across small patches of neural tissue the eigenfunctions are sinusoids and that simple Fourier techniques apply. This in fact is often the approach taken in experiment. Actually this approach is borne out by the above analysis. To see this we consider expression (16) in the neighborhood of an arbitrary reference point,

$$\psi \sim \mathcal{A}(q)\exp\left[\frac{i}{\epsilon}\int^q p(s)ds\right] = \exp[ip(\epsilon x_0)(x-x_0)] \times \left\{\mathcal{A}(\epsilon x)\exp\left[\frac{i}{\epsilon}\int_0^{\epsilon x_0} p(s)ds + 0(\epsilon)\right]\right\}. \quad (20)$$

The first factor on the right-hand side bears out the contention that ψ is locally a sinusoid. A problem in adopting this point of view is that it does not tell us how to connect the sinusoids on contiguous patches. Looking at the second factor on the right-hand side of Eq. (20), we see that this involves both a phase and an amplitude matchup. The approach that we have presented takes care of this problem in a natural way.

It is of interest at this point to mention studies of cortical or foveal magnification.[29–36] Such studies imply that the projection of the retina onto the visual cortex introduces a degree of homogeneity at the cortical level. It is of interest to observe that the WKB approach, by forcing the form of the eigenfunction into a sinusoid, expression (16), introduces a mapping, viz.,

$$Q = \int^q p(s)ds, \quad (21)$$

so that in the mapped space the description becomes homogeneous. This can be accomplished only to lowest order since the amplitude term in expression (16) in general must vary with position. This is reminiscent of the physiological observations of Dow *et al.*,[37] who, in an extension of earlier research, have shown that the apparent homogeneity is lost in the foveal projection region.

4. VISUAL EIGENFUNCTIONS

The construction of the eigenfunctions and determination of the eigenvalues follows from an analysis of the Wigner transform (17). For the retinal model given by Eq. (14) this is

$$\tilde{K}(p,q) = A_0\sqrt{\pi}\,\frac{1+|q|}{1+|q|/\kappa}(X - X^3), \quad (22)$$

where

$$X = \exp\left[-\frac{(1+|q|)^2}{4}p^2\right]. \quad (23)$$

With regard to the research of Wilson and Bergen,[19] the model (14) and its Wigner transform (22) apply to what they refer to as the N and S mechanisms. Table 1 indicates appropriate parameter values valid in the two cases.

In Figs. 1 and 2 we plot contour lines of Eq. (22) in these two instances. It is clear from the symmetry of Eq. (22) that only the first quadrant need be shown, since the full picture follows from reflection in coordinate axes. In these figures continuous lines represent closed contours and correspond to eigenvalues. The unclosed pair of continuous lines actually close at infinity and are asymptotic to the long-dashed curve. This pair represents the last closed curve and, as calculation shows, it contains an infinite area. The discrete eigenvalues, which lie in the range

$$\frac{2\kappa}{3\sqrt{3}} < \frac{\lambda}{A_0\sqrt{\pi}} < \frac{2}{3\sqrt{3}}, \quad (24)$$

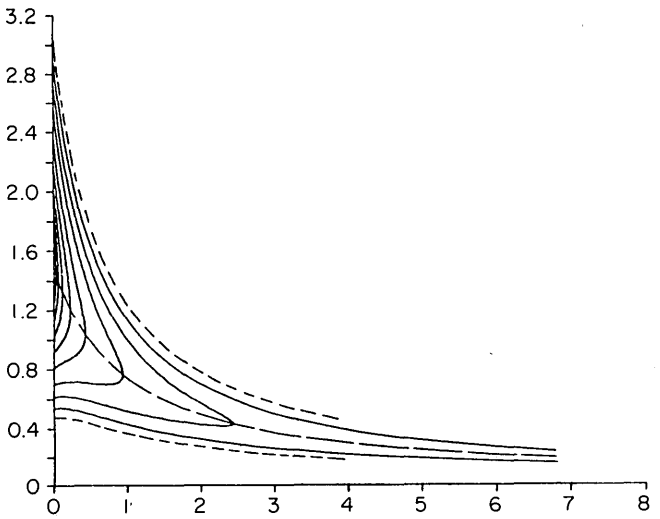

Fig. 1. Level lines of the Wigner transform, Eq. (17), of the retinal model (13), for the N mechanism. Only the first quadrant is shown. Complete contour lines are obtained by reflection in the vertical and horizontal axes.

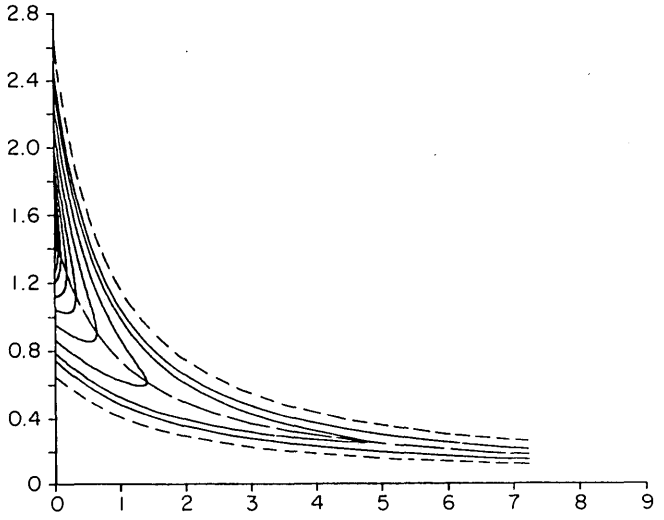

Fig. 2. Same as Fig. 1 except for the S mechanism.

are infinite in number and accumulate at $\lambda = (2\kappa A_0\sqrt{\pi})/3\sqrt{3}$. In addition to the discrete eigenvalues there is a continuous spectrum

$$0 < \frac{\lambda}{A_0\sqrt{\pi}} < \frac{2}{3\sqrt{3}}\kappa, \tag{25}$$

and the pair of short-dashed lines corresponds to a value of λ in this range.

The eigenfunctions of most importance in a psychophysical or physiological context are those that correspond to the largest eigenvalues. These will elicit the greatest responses, and thus a neural structure should be most sensitive to these. For the kernels under investigation, these correspond to the allowable curves closest to the peaks of $\tilde{K}(p, q)$ and thus correspond to the eigenfunctions of smallest indices. Such eigenfunctions are termed principal eigenfunctions. For such eigenfunctions, an improvement over the representation (16) may be obtained. Since this is somewhat technical we forgo such a discussion and simply state that these eigenfunctions may be more accurately represented in terms of Airy functions,[27] and plots discussed below were obtained from this representation.

Corresponding to each eigenvalue there are two eigenfunctions, one even and one odd. The first four eigenfunctions of the S mechanism are shown in Fig. 3. The abscissa is given in degrees, whereas the ordinate is arbitrary. All the eigenfunction patterns have been normalized to have a unit square integral.

A similar set of eigenfunctions can be exhibited for the N mechanism. As the values of σ in Table 1 indicate, the scaling is different in the two cases. To illustrate this difference, we have plotted in Fig. 4 the first eigenfunctions of the S and N mechanisms. This comparison suggests that each of these maximally sensitive stimuli is poorly matched to the neural mechanism of the other. In fact, the inner product of these two eigenfunctions is roughly 0.01.

The underlying spatial frequency of the S mechanism is found to be 3.6 cycles/deg, whereas that of the N mechanism is 7.2 cycles/deg. In this connection we mention the recent study by Watson *et al.*[38] in which a best pattern is sought and is found to have an underlying spatial frequency of roughly 7 cycles/deg. In view of the diversity of treatments this general agreement can be regarded as quite encouraging. There is, however, a disquieting aspect to this compari-

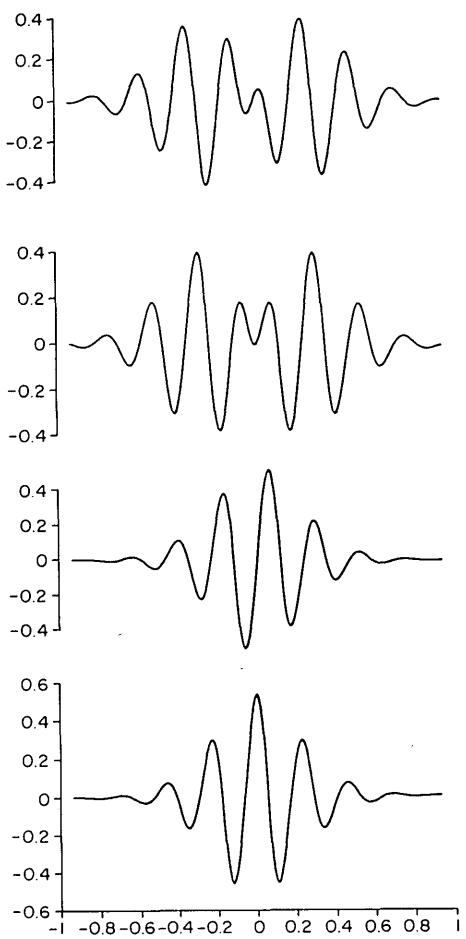

Fig. 3. First four eigenfunctions of the S mechanism, to be read from bottom to top. Abscissa in degrees and ordinate in arbitrary units.

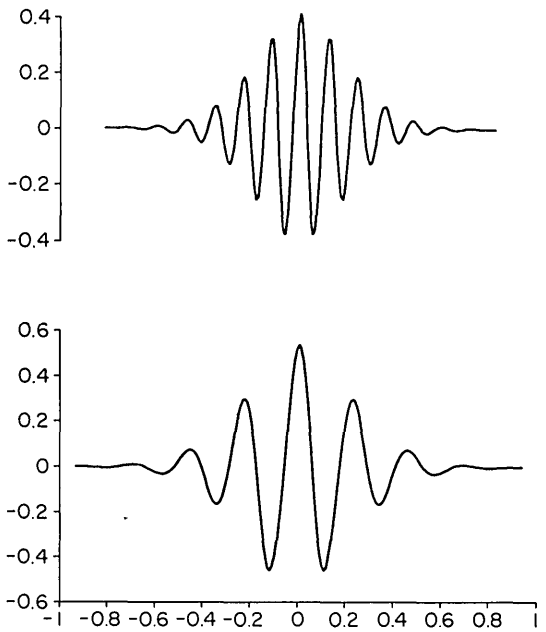

Fig. 4. Comparison of first eigenfunctions of the S mechanism (lower) and the N mechanism (upper).

son. An accurate estimate of the relative sensitivity of each mechanism is given by the product $A_0\sigma$; thus Table 1 then implies that the S mechanism is almost three times as sensitive as the N mechanism. From the research of Wilson and Bergen[19] we see that the S mechanism was not explicitly measured. Rather, it is what is left after the channels have been determined. This commentary on the model suggests that further research is necessary.

5. THE TWO-DIMENSIONAL RETINA

Although the above treatment follows from a general formalism, it depends for particular details on the results of Wilson and Bergen[19]. In using their or any line-spread function one is at best approximating the true physical situation. In the present section we attempt to give this some perspective by generalizing the discussion to the two-dimensional retina.

Although most of the remarks in this section apply to general retinal models, it will be convenient to deal with the following somewhat specific model of a point-spread function:

$$K\{\mathbf{x},\mathbf{y}\} = A(q)\left\{\exp\left[-\frac{(\mathbf{x}-\mathbf{y})^2}{d_1^2(q)}\right] - B\exp\left[-\frac{(\mathbf{x}-\mathbf{y})^2}{d_2^2(q)}\right]\right\}, \tag{26}$$

where

$$q = \epsilon\left|\frac{\mathbf{x}+\mathbf{y}}{2}\right| \tag{27}$$

and $\mathbf{x} = (x_1, x_2)$ and $\mathbf{y} = (y_1, y_2)$ are each two-component vectors. The kernel, Eq. (26), represents a center-surround opponent mechanism based on the collection areas d_1^2 and d_2^2 and a sensitivity measured by $A(q)$. In writing K in the form of Eq. (26) we adopt our earlier normalization, Eq. (12), so that ϵ again measures the (slow) departure from homogeneity, and $\mathbf{x}$ and $\mathbf{y}$ have been made dimensionless with respect to a characteristic space constant. Within certain bounds we will show that Eq. (26) may be reduced to Eq. (14) for one-dimensional patterns.

From measurements of resolution versus eccentricity[39–41] there is strong evidence that outside the fovea the collection radius d in Eq. (26) varies directly with distance. Thus we take

$$d_1 = 1 + \epsilon\left|\frac{\mathbf{x}+\mathbf{y}}{2}\right| = 1 + q = d. \tag{28}$$

In general both collection areas, d_1^2 and d_2^2, may vary independently, but for simplicity and in keeping with the one-dimensional model, Eq. (14), we take

$$d_2 = 3d. \tag{29}$$

Although data exist on which to base the form of A in Eq. (26), there is some disagreement. Evidence for the form taken by A comes primarily from experiments on sensitivity versus eccentricity. Shapley[42] and Fischer and May[41] find that A should fall off with the inverse square of distance, whereas Linsenmaier *et al.*[43] suggest a less rapid falloff. As we now show, the model of Eq. (14) is consistent with the inverse square falloff.

To derive the one-dimensional kernel (14) from Eq. (26), we recall the circumstances under which Eq. (14) was determined.[19] A stimulus pattern varying in only the x_1 direction appeared in a slot that subtended 1.5 deg vertically and 8 deg horizontally across the fovea. It thus appears that the slot's vertical extent is quite large compared with the *collection radius* d over the full horizontal range of the illuminated slot. It follows that the equivalent one-dimensional kernel (line-spread function) is

$$K_1 = \int_{y_2<D/2\sigma} K\{x, y\}\mathrm{d}y_2, \tag{30}$$

where the limits of integration in this form take into consideration the normalization, Eqs. (12), and the height of the slot (D = 1.5 deg). It is then a simple calculation to show that this is well approximated by

$$K_1 \approx \sqrt{\pi}A(q)\mathrm{d}\left\{\exp\left[-\frac{(x_1-y_1)^2}{d^2}\right] - B\sqrt{3}\exp\left[-\frac{(x_1-y_1)^2}{3d^2}\right]\right\}. \tag{31}$$

In view of the limited range in the vertical direction we can to good approximation put $x_2 \approx 0$, where it occurs in d in the above, and hence

$$d \approx 1 + \frac{\epsilon}{2}|x_1 + y_1|. \tag{32}$$

On comparison with Eq. (14) we take $B = 1/3$.

A comparison of the amplitude coefficient of expression (31) with Eq. (14) implies that $A(q)$ is $0(q^{-2})$ for large q, as mentioned earlier. If also

$$A(q) = \frac{A_0}{\sqrt{\pi}(1+\epsilon\mu q)^2}, \tag{33}$$

then the one-dimensional form, Eq. (27), becomes

$$K_1 = \frac{A(1+q)}{(1+\epsilon\mu q)^2}\left\{\exp\left[-\frac{(x-y)^2}{d^2}\right] - \frac{1}{\sqrt{3}}\exp\left[-\frac{(x-y)^2}{3d^2}\right]\right\}. \tag{34}$$

For a suitable choice of μ in Eq. (34) there is little discernible difference in the amplitude functions of Eqs. (14) and (34). Wilson and Bergen[19] present data at only three eccentricities, and as a result there would be little to distinguish Eq. (34) and Eq. (14). The eigenfunction analysis of the former does not differ significantly from that of the latter and so will not be presented. In the same vein we mention that other reasonable functional forms for both A and d also lie within the experimental data of Wilson and Bergen. In particular we mention that $d^2 = 1 + q^2$, $A = (1 + \chi q^2)^{-1}$ (for suitable χ) leads to a model of interest.

An analysis of characteristic functions for the fully two-dimensional form (26) may also be performed. Although it is too lengthy to be presented here, one result bears mentioning. If the falloff in the sensitivity $A(q)$ in Eq. (26) is less rapid than $0(q^{-2})$, the retina will always be most sensitive to illumination patterns of relatively low spatial frequency and restricted to the periphery. With regard to most-sensitive patterns, a retina organized in this way is qualitatively different from what we have explored above. Thus our methodology furnishes an incentive and perhaps a means to investigate further the tentative slow falloff observations of Linsenmeir *et al.*[43]

Finally, it should be noted that temporal effects have been ignored in the above treatment. This is of some importance but requires a greatly extended analysis. Such a treatment is now in preparation.

ACKNOWLEDGMENTS

We gratefully acknowledge our debt to Robert Shapley for many helpful discussions. This research was supported by the National Science Foundation under grant MCS-77-08598 and the U.S. Eye Institute under grants EY 188, EY 1428, and EY 1472.

L. Sirovich is also with the Division of Applied Mathematics, Brown University, Providence, Rhode Island 02912.

REFERENCES

1. F. W. Campbell and J. G. Robson, "Application of Fourier analysis to the visibility of gratings," J. Physiol. (London) **197,** 551–566 (1968).
2. N. Graham and J. Nachmias, "Detecting of grating patterns containing two spatial frequencies: A comparison of single and multiple channel models," Vision Res. **11,** 251–261 (1971).
3. J. Robson, "Receptive fields: neural representation of the spatial and intensive attributes of visual image," in *Seeing,* E. Cartenette and M. S. Friedman, eds., Vol. 5 of Handbook of Perception (Academic, New York, 1975).
4. F. Ratliff, *Mach Bands: Quantitative Studies on Neural Networks in the Retina* (Holden-Day, San Francisco, Calif., 1965).
5. V. Volterra, *Theory of Functionals and of Internal and Integrodifferential Equations* (Blackie and Sons, London, 1959).
6. S. E. Brodie, B. W. Knight, and F. Ratliff, "The response of the limulus retina to moving stimuli. A prediction by Fourier synthesis," J. Genet. Physiol. **72,** 129–166 (1978).
7. S. E. Brodie, B. W. Knight, and F. Ratliff, "The spatiotemporal transfer function of the Limulus lateral eye," J. Genet. Physiol. **72,** 167–202 (1978).
8. L. S. Sirovich, S. E. Brodie, and B. W. Knight, "The effect of boundaries on the response of a neural network," Biophys. J. **28,** 423–446 (1979).
9. L. Sirovich, "Boundary effects in neural networks," SIAM J. Appl. Math. **39,** 142–160 (1980).
10. P. M. Duffieux, *L'Integrale de Fourier et ses Applications à L'Optique* (Societé anonyme Oberthur, Rennes, 1946).
11. O. H. Schade, "Optical and photoelectric analog of the eye," J. Opt. Soc. Am. **46,** 721–739 (1956).
12. F. W. Campbell and D. G. Green, "Optical and retinal factors affecting visual resolution," J. Physiol. (London) **181,** 576–593 (1965).
13. J. J. Kulikowski, "Effective contrast constancy and linearity of contrast sensation," Vision Res. **16,** 1419–1431 (1976).
14. M. A. Georgeson and G. D. Sullivan, "Contrast constancy: deblurring in human vision by spatial frequency channels," J. Physiol. (London) **252,** 627–656 (1975).
15. J. Gottesman, G. S. Ruben, and G. E. Legge, "A power law for perceived contrast in human vision," Vision Res. **21,** 791–799 (1981).
16. M. W. Cannon, "Contrast sensation: a linear function of stimulus contrast," Vision Res. **19,** 1045–1052 (1979).
17. A. P. Ginsburg, M. W. Cannon, and M. A. Nelson, "Suprathreshold processing of complex visual stimuli: evidence for linearity in contrast perception," Science **208,** 619–621 (1980).
18. H. Wilson, "Qualitative characterization of two types of line-spread function near the fovea," Vision Res. **18,** 971–981 (1978).
19. H. R. Wilson and J. R. Bergen, "A four mechanism model for threshold spatial vision," Vision Res. **19,** 19–32 (1979).
20. J. Q. Limb and C. B. Rubinstein, "A model of threshold vision incorporating inhomogeneity of the visual field," Vision Res. **17,** 571–584 (1977).
21. M. Hines "Line spread function variation near the fovea," Vision Res. **16,** 567–572 (1976).
22. G. F. Legge, "Space domain properties of a spatial frequency channel in human vision," Vision Res. **18,** 959–969 (1978).
23. J. G. Robson and N. Graham, "Probability summation and regional variation in contrast sensitivity across the visual field," Vision Res. **21,** 409–418.
24. L. Sirovich, *Techniques of Asymptotic Analysis* (Springer-Verlag, New York, 1971).
25. J. Heading, *An Introduction to Phase Integral Methods* (Wiley, New York, 1962).
26. L. Sirovich and B. W. Knight, "On the eigentheory of operators which exhibit a slow variation," Q. Appl. Math. **38,** 469–488 (1981).
27. L. Sirovich and B. W. Knight, "Contributions to the eigenvalue problem for slowly varying operators," SIAM J. Appl. Math. **42,** 356–377 (1982).
28. B. W. Knight and L. Sirovich, "The Wigner transform and some exact properties of linear operators," SIAM J. Appl. Math. **42,** 378–389 (1982).
29. P. M. Daniel and D. Whitteridge, "The representation of the visual field on the cerebral cortex in monkeys," J. Physiol. (London) **159,** 203–221 (1961).
30. A. Cowey and E. T. Rolls, "Human cortical magnification factor and its relation to visual acuity," Exp. Brain Res. **21,** 447–454 (1974).
31. D. H. Hubel and T. N. Wiesel, "Uniformity of monkey straite cortex: a parallel relationship between field size, scatter, and magnification factor," J. Comp. Neurol. **158,** 295–305 (1974).
32. N. Drasdo, "The neural representation of visual space," Nature **266,** 554–556 (1977).
33. J. Ravamo, V. Virsu, and R. Nasanen, "Cortical magnification factor predicts the photopic contrast sensitivity of peripheral vision," Nature **271,** 54–56 (1978).
34. J. Rovamo and V. Virsu, "An estimation and application of the human cortical magnification factor," Exp. Brain Res. **37,** 495–510 (1979).
35. V. Virsu and J. Rovamo, "Visual resolution, contrast sensitivity, and the cortical magnification factor," Exp. Brain Res. **37,** 495–510 (1979).
36. R. B. H. Tootell, M. S. Silverman, E. Switkes, and R. L. De Valois, "Deoxyglucose analysis of retinotopic organization in primate straite cortex," Science **218,** 902–904 (1982).

37. B. M. Dow, A. Z. Snyder, R. G. Vautin, and R. Bauer, "Magnification factor and receptive field size in foveal straite cortex of the monkey," Exp. Brain Res. **44,** 213–228 (1981).
38. A. B. Watson, H. B. Barlow, and J. G. Robson, "What does the eye see best?" Nature **302,** 419–422 (1983).
39. Y. T. So and R. M. Shapley, "Spatial properties of *X* and *Y* cells in the lateral geniculate nucleus of the cat and conduction velocities of their inputs," Exp. Brain Res. **36,** 533–550 (1979).
40. B. G. Cleland, T. H. Harding, and U. Tulunay-Keesey, "Visual resolution and receptive field size: examination of two kinds of retinal ganglion cells," Science **205,** 1015–1017 (1979).
41. B. Fischer, and H. U. May, "Invarianzen in der Katzen Retina: Gesetzmassige Beziehungen Zwischen Empfindlichkeit, grosse und lage receptivier Felder von Ganglienzellen," Exp. Brain Res. **11,** 448–464 (1970).
42. R. Shapley, Rockfeller University, New York, N.Y. 10021 (personal communication, 1982).
43. R. A. Linsenmaier, L. J. Frishman, H. G. Jakiela, and C. Enroth-Cugell, "Receptive field properties of *x* and *y* cells in the cat retina derived from contrast sensitivity measurements," Vision Res. **22,** 1173–1185 (1982).